MHD FREE CONVECTION OF NON-NEWTONIAN POWER-LAW FLUIDS OVER A UNIFORMLY HEATED HORIZONTAL PLATE

Alireza Bahmani[1], Hadi Kargarsharifabad[1,2*]

[1]Department of Mechanical Engineering, Semnan Branch, Islamic Azad University, Semnan, Iran.

[*2]Energy and Sustainable Development Research Center, Islamic Azad University, Semnan, Iran.

[*] Corresponding author; E-mail: h.kargar@semnaniau.ac.ir

The magnetohydrodynamic free convection flow of non-Newtonian power-law fluids over a horizontal plate subjected to a constant heat flux is studied. The results are presented for various values of the three influential parameters, i.e. the generalized Hartmann number (Ha^*), the generalized Prandtl number (Pr^*), and the non-Newtonian power-law viscosity index (n). Increasing the Hartmann number increases the thermal boundary layer thickness and the surface temperature and consequently decreases the wall skin friction and Nusselt number. A lower Pr^* results in a larger skin friction coefficient and higher wall temperature as well as thicker thermal boundary layer. The viscosity index (n) is predicted to influence the flow conditions depending on the value of Pr^*. At high Pr^* numbers, by decreasing n, the wall skin friction, temperature scale, and thermal boundary layer thickness are increased and the Nusselt number is decreased, while the opposite trend is observed for low Pr^*. A general correlation for the Nusselt number is derived using the numerical results.

Key words*: Horizontal plate; Magnetohydrodynamics (MHD); Natural convection; Non-Newtonian; Power-law fluid; Similarity solution.*

1. Introduction

The buoyancy-driven convection has important applications in many engineering and industrial processes such as nuclear reactors, biochemical processes, drying systems, etc. The free convective boundary layer flows over flat surfaces have been extensively investigated [1]. In contrast, the natural convection flow and heat transfer over horizontal plates had received fewer attentions. The boundary layer above a heated horizontal plate is formed by an induced pressure gradient resulted from the buoyancy force perpendicular to the plate. Thus, the mechanism of natural convection flow over horizontal heated surfaces is different from the vertical ones. A numerical and experimental investigation of natural convection flow above a horizontal plate heated with a constant flux has been reported in [2]. Samie et al. [3] analytically analyzed the natural convection heat transfer below a hot horizontal isothermal flat strip of infinite length. Kozanoglu and Rubio [4] introduced a Nusselt number correlation for the natural convection from a downward facing horizontal heated plate in which the characteristic length is defined based on the thermal boundary layer thickness. The natural convection flows over a semi-infinite horizontal plate subjected to variable heat flux or variable wall temperature have been presented in [5,6]. Guha and Samanta [7] performed an integral analysis to

investigate natural convection heat transfer over a semi-infinite horizontal plate subjected to either a variable wall temperature or variable heat flux.

Many industrial fluids such as petroleum products, polymers, molten plastics, and slurries are known to have non-Newtonian characteristics in which the shear rate is not directly proportional to the shear stress. The non-Newtonian behavior of these fluids mostly exhibits itself by a shear-dependent viscosity. Due to the growing use of such fluids, the phenomenon of natural convection has been widely investigated for the flow of these types of fluid on vertical [8-12], inclined [13], and horizontal surfaces [14-18]. Different studies have been reported on the steady natural convection flow of power-law fluids over vertical surfaces with constant temperature [8], constant wall heat flux [9,10], and under mixed thermal boundary conditions [11]. The problem of unsteady free convection flow over a vertical flat plate at constant temperature immersed in a power-law fluid is analyzed in [12]. The free convection of non-Newtonian fluids over an inclined plate with variable surface temperature is studied in [13], where the effects of power-law viscosity and suction/injection through the surface have been investigated.

A similarity solution of natural convection of non-Newtonian power-law fluid about a horizontal impermeable surface with a nonuniform heat flux distribution in the porous medium has been reported in [14]. In addition, Gorla and Kumari [15] have investigated free convection problem for the horizontal plate subject to variable wall temperature or heat flux distribution embedded in non-Newtonian power-law fluid-saturated porous media. In their work, the effects of surface mass transfer was studied for different conditions employing finite difference approach to solve the transformed boundary layer equations. Guha and Pradhan [16] used the finite difference method to study the problem of natural convection boundary layer flow of a non-Newtonian power-law fluid over an isothermal horizontal plate. Their results showed that the hydrodynamic boundary layer is influenced by the non-Newtonian nature of fluid while the thermal boundary layer remains almost unaffected for a given generalized Prandtl number.

The flow of electrically conducting fluids, e.g., liquid metals, suppress under the influence of magnetic fields. This effect, the magnetohydrodynamic (MHD) phenomenon, is widely used to control the heat transfer processes of electrically conducting fluids [17,18]. Subsequently, MHD can mitigate or neutralize the development of flow instabilities [19-21]. Many researchers have studied the MHD natural convection flow and heat transfer on a plate. The effect of magnetic fields on natural convection flow past vertical or inclined plates are extensively studied [22-26]. The buoyancy-induced flow over horizontal plates embedded in a non-Newtonian fluid saturated porous medium under the action of a transverse magnetic field is investigated in [26,27]. Samanta and Guha [28] studied the natural convection of an electrically conducting fluid above a horizontal plate with constant heat flux in the presence of a magnetic field. The results of magnetic field effect in reducing the Nusselt number and skin friction coefficient was presented.

The objective of the present study is to investigate the effects of a transverse magnetic field on natural convection flow and heat transfer of an electrically conducting non-Newtonian fluid over a semi-infinite horizontal plate heated with constant heat flux. The similarity transformations are applied to the governing boundary layer equations to reduce them to a set of ordinary differential equations. A numerical solution using the finite difference method is obtained. The effect of the generalized Hartmann number on the non-dimensional velocity and temperature fields in both shear-thinning and

shear-thickening fluids are then presented and discussed. Finally, using the results of numerical solutions, a general correlation for Nusselt number is proposed.

2. Mathematical analysis

A semi-infinite horizontal plate situated in a quiescent ambient of non-Newtonian power-law fluid at a uniform temperature T_∞ and pressure p_∞ is considered. As shown in Fig. 1, the plate is heated with a constant heat flux q_w and is subjected to a unidirectional magnetic field B normal to the plate. Above the heated plate, a natural convection boundary layer is formed due to an induced pressure gradient. The problem under consideration is the steady two-dimensional laminar incompressible natural convection boundary layer flow and heat transfer over the plate.

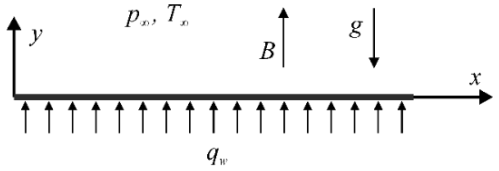

Fig. 1. Schematic representation of the problem.

The governing equations of MHD natural convection flow over a horizontal surface are presented in Eq. (1). In addition to the previously mentioned assumptions, the Boussinesq and boundary layer approximations are applied. The x-coordinate is aligned along the plate from the leading edge and the y-coordinate is directed perpendicular to the plate.

$$\frac{\partial u}{\partial x}+\frac{\partial v}{\partial y}=0 \tag{1a}$$

$$u\frac{\partial u}{\partial x}+v\frac{\partial u}{\partial y}=-\frac{1}{\rho}\frac{\partial p}{\partial x}+\frac{1}{\rho}\frac{\partial}{\partial y}\left(\mu\frac{\partial u}{\partial y}\right)-\frac{\sigma B^2}{\rho}u \tag{1b}$$

$$0=-\frac{1}{\rho}\frac{\partial p}{\partial y}+g\beta(T-T_\infty) \tag{1c}$$

$$u\frac{\partial T}{\partial x}+v\frac{\partial T}{\partial y}=\alpha\frac{\partial^2 T}{\partial y^2} \tag{1d}$$

The third term on the right-hand side of Eq. (1b) represents the Lorentz force, $\vec{j}\times\vec{B}$ obtained by the simplification of one-dimensional magnetic field. The magnetic Reynolds number was assumed small and the induced magnetic field due to the motion of the electrically conducting fluid was neglected. The appropriate boundary conditions for Eq. (1) are

$$\text{at}\ \ y=0,\ \ u=0,\ \ v=0,\ \ -k\partial T/\partial y=q_w \tag{2a}$$

$$\text{at}\ \ x=0,\ \ u=0,\ \ v=0,\ \ T=T_\infty \tag{2b}$$

$$\text{as}\ \ y\to\infty,\ \ u\to 0,\ \ T\to T_\infty,\ \ P\to p_\infty \tag{2c}$$

In the above equations, u and v are the velocity components in the x- and y- directions, respectively; p is the hydrostatic pressure; T is the static temperature of the fluid; g is the gravitational acceleration; β is the volumetric coefficient of thermal expansion; and ρ, μ, α and σ are the density, viscosity, thermal diffusivity, and electrical conductivity of the fluid, respectively.

The continuity Eq. (1a) is automatically satisfied by introducing a stream function ψ, defined by $u=\partial\psi/\partial y$ and $v=-\partial\psi/\partial x$. Then, the governing equations can be expressed as

$$\frac{\partial\psi}{\partial y}\frac{\partial^2\psi}{\partial x\partial y}-\frac{\partial\psi}{\partial x}\frac{\partial^2\psi}{\partial y^2}=-\frac{1}{\rho}\frac{\partial p}{\partial x}+\frac{\mu_0}{\rho}\frac{\partial}{\partial y}\left(\left|\frac{\partial^2\psi}{\partial y^2}\right|^{n-1}\frac{\partial^2\psi}{\partial y^2}\right)-\frac{\sigma B^2}{\rho}\frac{\partial\psi}{\partial y} \tag{3a}$$

$$0 = -\frac{1}{\rho}\frac{\partial p}{\partial y} + g\beta(T - T_\infty) \tag{3b}$$

$$\frac{\partial \psi}{\partial y}\frac{\partial T}{\partial x} - \frac{\partial \psi}{\partial x}\frac{\partial T}{\partial y} = \alpha\frac{\partial^2 T}{\partial y^2} \tag{3c}$$

where the power-law model is used to describe the shear dependent viscosity behavior of the fluid. In this non-Newtonian model, the viscosity is assumed to be a function of shear rate as $\mu = \mu_0|\partial u/\partial y|^{n-1}$, where n is a fluid property and is constant for a given fluid. The shear-thinning fluids (n < 1) have lower apparent viscosity at higher shear rates while in shear-thickening fluids (n > 1) there is an increase in the apparent viscosity at higher shear rates. In Newtonian fluids, the shear stress is directly proportional to the shear rate (i.e., n = 1).

The group theory analysis [29] provides that the following combinations of the variables give the absolute invariants:

$$y/x^{\frac{1}{3}},\ \psi/x^{\frac{2}{3}},\ (T - T_\infty)/x^{\frac{1}{3}},\ (P - P_\infty)/x^{\frac{2}{3}},\ B/x^{-\frac{1}{3}} \tag{4a}$$

Therefore, the similarity transformations can then be written as

$$\eta = Dyx^{-\frac{1}{3}},\ \psi = C_1x^{\frac{2}{3}}F(\eta),\ (T - T_\infty) = C_2x^{\frac{1}{3}}G(\eta),\quad (P - P_\infty) = C_3x^{2/3}H(\eta),\ B = B_0x^{-1/3}M(\eta) \tag{4b}$$

where D, C_1, C_2, C_3, and B_0 are constants. Hence, there exist similarity solutions to this problem for a magnetic field with $M = Bx^{1/3}/B_0$ as a η function. As long as the direction of the magnetic field is normal to the plate, the simplified presented form of Lorentz force is valid. By letting $M(\eta) = \text{constant}$, in this paper, a non-uniform magnetic field as $B = B_0D^{-1/2}x^{-1/3}$ is investigated. By using the definition of η, we define a length scale as $L = D^{-3/2}$. Hence, the constant value of $M(\eta)$ is chosen as $D^{-1/2}$ to maintain the dimension of B as Tesla.

By substituting the similarity transformations Eq. (4b) into Eq. (3), the boundary layer equations are transformed into the following set of ordinary differential equations:

$$\frac{C_1^2D^2}{3}\left[F'^2(\eta) - 2F(\eta)F''(\eta)\right] = -\frac{C_3}{3\rho}[2H(\eta) - \eta H'(\eta)] + \frac{n\mu_0C_1^nD^{2n+1}}{\rho}[|F''(\eta)|^{n-1}F'''(\eta)] - \frac{C_1\sigma B_0^2}{\rho}F'(\eta) \tag{5a}$$

$$-\frac{C_3D}{\rho}H'(\eta) + g\beta C_2G(\eta) = 0 \tag{5b}$$

$$\frac{C_1C_2D}{3}[F'(\eta)G(\eta) - 2F(\eta)G'(\eta)] = \alpha C_2D^2G''(\eta) \tag{5c}$$

where the prime sign denotes differentiation with respect to η. Also, the heat flux boundary condition implies that $-kC_2DG'(0) = q_w$. The transformed governing equations and the associated transformed boundary conditions may be written as

$$3n|F''|^{n-1}F''' + 2FF'' - F'^2 - \mathrm{Ha}^{*2}F' + \eta H' - 2H = 0 \tag{6a}$$

$$H' - G = 0 \tag{6b}$$

$$\frac{3}{\mathrm{Pr}^*}G'' + 2FG' - F'G = 0 \tag{6c}$$

$$F(0) = F'(0) = G'(0) + 1 = F'(\infty) = G(\infty) = H(\infty) = 0 \tag{6d}$$

with an appropriate choice of constants as

$$D = \left[\frac{g\beta q_w}{k\nu_0^{\frac{2}{2-n}}}\right]^{\frac{2-n}{6}},\quad C_1 = \left[\frac{g\beta q_w}{k\nu_0^{\frac{-4}{2n-1}}}\right]^{\frac{2n-1}{6}},\quad C_2 = \frac{q_w}{k}\left[\frac{g\beta q_w}{k\nu_0^{\frac{2}{2-n}}}\right]^{\frac{n-2}{6}},\quad C_3 = \rho\left[\frac{g\beta q_w}{k\nu_0^{\frac{-2}{n+1}}}\right]^{\frac{n+1}{3}} \tag{7}$$

Then, the generalized Hartmann number Ha^* and Prandtl number Pr^* appeared in Eqs. (6a) and (6c), respectively, are given by

$$\mathrm{Ha}^* = B_0\sqrt{\frac{\sigma}{\rho C_1 D^2}} = B_0\left(\frac{g\beta q_w}{k}\right)^{-\frac{1}{4}}\sqrt{\frac{\sigma}{\rho}} = B_0 L\sqrt{\frac{\sigma}{\rho\nu^*}},$$
$$\mathrm{Pr}^* = \frac{C_1}{\alpha D} = \frac{\nu^*}{\alpha},\quad \nu^* = \nu_0\left(\frac{g\beta q_w}{k}\right)^{\frac{n-1}{2}} \tag{8}$$

where $L = D^{-3/2}$ is the characteristic length scale. The generalized kinematic viscosity ν^* reduces to $\nu_0 = \mu_0/\rho$ for n = 1. Here, the parameter ν_0 is dimensionless only for n =1, but ν^* is dimensionless for all n.

Using Eq. (7), the similarity transformations can be determined as

$$\eta = \frac{y}{x}\mathrm{Gr}_x^{*\frac{2-n}{6}}, \tag{9a}$$
$$\psi = (\nu_0 x^{2-2n})^{\frac{1}{2-n}}\,\mathrm{Gr}_x^{*\frac{2n-1}{6}}F(\eta), \tag{9b}$$
$$(T - T_\infty) = \frac{q_w x}{k}\mathrm{Gr}_x^{*\frac{n-2}{6}}G(\eta), \tag{9c}$$
$$(P - P_\infty) = \rho\left(\frac{\nu_0}{x^n}\right)^{\frac{2}{2-n}}\mathrm{Gr}_x^{*\frac{n+1}{3}}H(\eta) \tag{9d}$$
$$B = B_0 Gr_x^{*\frac{n-2}{12}} \tag{9e}$$

where the generalized Grashof number Gr_x^* is introduced as ($n \neq 2$)

$$\mathrm{Gr}_x^* = \frac{g\beta q_w x^{\frac{4}{2-n}}}{k\nu_0^{\frac{2}{2-n}}} \tag{10}$$

From the similarity transformation of stream function Eq. (9b), dimensionless transformed velocities can be obtained as

$$\frac{u}{\left(\frac{\nu_0}{x^n}\right)^{\frac{1}{2-n}}\mathrm{Gr}_x^{*\frac{n+1}{6}}} = u^* = F'(\eta), \tag{11a}$$
$$\frac{v}{\left(\frac{\nu_0}{x^n}\right)^{\frac{1}{2-n}}\mathrm{Gr}_x^{*\frac{2n-1}{6}}} = v^* = \frac{\eta}{3}F'(\eta) - \frac{2}{3}F(\eta) \tag{11b}$$

Using the similarity transformation of temperature Eq. (9c), the normalized local Nusselt number (Nu_x^*) can be expressed as

$$\mathrm{Nu}_x^* = \frac{\mathrm{Nu}_x}{\mathrm{Gr}_x^{*\frac{2-n}{6}}} = \frac{q_w x}{k(T_w(x) - T_\infty)\mathrm{Gr}_x^{*\frac{2-n}{6}}} = \frac{1}{G(0)} \tag{12}$$

Then, the average Nusselt number over a length of L is $\overline{\mathrm{Nu}}_{0-L} = 1.5\mathrm{Nu}_L$, where Nu_L is the local Nusselt number at $x = L$.

The wall shear stress is given by

$$\tau_w = \mu_0\left[\frac{\partial u}{\partial y}\bigg|_{y=0}\right]^n = \mu_0\left[\left(\frac{g\beta q_w}{k}\right)^{\frac{1}{2}}F''(0)\right]^n = \rho\left(\frac{\nu_0}{x^n}\right)^{\frac{2}{2-n}}\mathrm{Gr}_x^{*\frac{n}{2}}[F''(0)]^n \tag{13}$$

The wall shear stress τ_w is constant all over the surface of the plate. Using the u-velocity scale Eq. (11a), the normalized skin-friction coefficient ${c_f}_x^*$ can be defined as

$${c_f}_x^* = \frac{{c_f}_x}{\mathrm{Gr}_x^{*\frac{n-2}{6}}} = \frac{\tau_w}{\rho\left(\frac{\nu_0}{x^n}\right)^{\frac{2}{2-n}}\mathrm{Gr}_x^{*\frac{n+1}{3}}\mathrm{Gr}_x^{*\frac{n-2}{6}}} = [F''(0)]^n \tag{14}$$

3. Results and discussion

The system of coupled Eqs. (6a)-(6c) subject to boundary conditions Eq. (6d) have been solved numerically using finite-difference method. Equations (6a)-(6c) were first reduced to a system of six ordinary differential equations with appropriate boundary conditions. The central difference discretization scheme was applied to the partial derivatives to obtain the finite difference equations. The algebraic equations have been linearized by employing Newton–Raphson procedure. The iterative Thomas algorithm was used to solve the system of algebraic equations with a convergence criterion of 10^{-10} for relative difference between the current and previous iterations. The far-field asymptotic value of similarity variable η_∞ was increased till the unknown solutions at $\eta = 0$ and $\eta = \eta_\infty$ attained unchanged values within a tolerance of 10^{-8}. In the computational domains associated to each η_∞, the solution was supposed to be independent of the mesh size when the relative changes of the numerical results were less than 10^{-4} when doubling the number of grids.

The effect of magnetic field on the dimensionless *u*-velocity profiles for three different values of the generalized Prandtl number Pr^* = 0.1, 1, and 10 is presented in Fig. 2 for a pseudo plastic fluid with n = 0.5, Newtonian fluids (n = 1) and a dilatant fluid with n = 1.5. As expected, Fig. 2 shows that the maximum value of dimensionless *u*-velocity decreases with the increase of the generalized Hartmann number or Prandtl number. Furthermore, the location of maximum *u*-velocity approaches the leading edge with the increase of the generalized Hartmann number. Generally, increasing the Hartmann number increases the boundary layer thickness; but, opposite trend was seen when low Hartmann numbers are applied for the cases with thick boundary layers at high Pr^* and low n values.

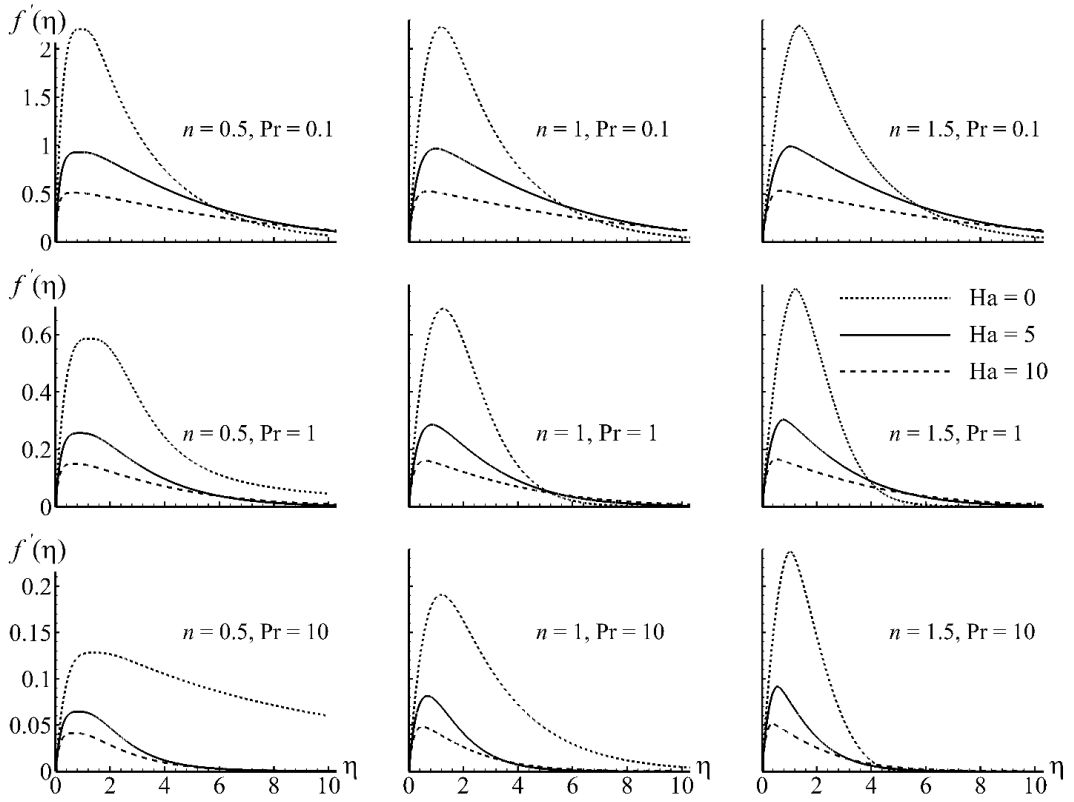

Fig. 2. Dimensionless *u*-velocity distribution for different n and Pr^* for Ha^* = 0, 5, and 10.

As can be seen in Fig. 2, a thicker boundary layer is resulted for a larger Pr^* number. It is observed that a larger n results in a larger and sharper peak velocity but a thinner boundary layer thickness. These can be explained by the fact that the effective viscosity decreases in shear-thickening fluids and increases in the shear-thinning fluids by the decrease in the velocity gradient. The low velocity gradients near the point of the maximum velocity produce low effective viscosities for shear-thickening fluids, which result in higher velocities with sharper variations. In comparison with Newtonian fluids, by the decrease in the shear rate starting from the plate surface to the boundary layer edge, the viscous effects are presented in a thicker boundary layer for shear-thinning fluids and a thinner boundary layer for shear-thickening fluids.

The dimensionless wall skin friction is plotted against generalized Hartmann number in Fig. 3. As can be seen, increasing the Hartmann number decreases the friction coefficient. This is evident that higher values of generalized Hartmann or Prandtl number result in the smaller velocity scales (Fig. 2), and thus lower values of normalized skin friction regardless of the value of n. Fig. 3 shows that for $Pr^* = 10$, the dimensionless skin friction coefficient varies slightly with Hartmann number. Equivalently, the velocity gradient near the surface have a weak functionality of Hartmann number at $Pr^* = 10$.

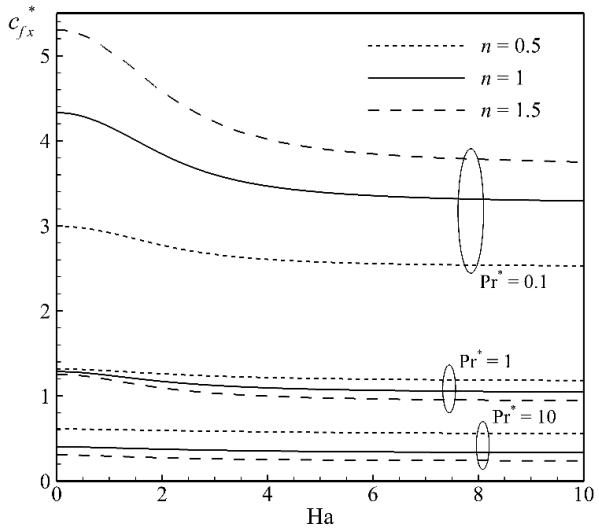

Fig. 3. The dimensionless skin friction factor versus Ha number for different values of Pr^* and n.

Fig. 3 indicates that the wall skin friction decreases with n for $Pr^* = 10$, while the reverse happens for $Pr^* = 0.1$. As discussed earlier, increasing n at a fixed Pr^* results in a higher peak velocity (Fig. 2) but a thinner momentum boundary layer thickness. The former and the latter both may reveal an increase in the velocity gradient $F''(\eta)$. The aforesaid comment is consistent for $Pr^* = 10$; but considering the effect of the power index n on the effective viscosity, an apparently contradictory result is obtained for $Pr^* = 0.1$, where the velocity gradients has decreasing trends with increase in index n. On the other hand, by raising the values of the dimensionless velocity gradients at the wall to the power of n in order to obtain the skin friction, different trends for variations of $\left[F''|_{\eta=0}(n)\right]^n$ are established depending on the value of $F''|_{\eta=0}$ and n.

The effect of magnetic field on the dimensionless temperature profiles is presented in Fig. 4 for three different values of generalized Prandtl number $Pr^* = 0.1$, 1, and 10 for $n = 0.5$, 1, and 1.5. The value of the dimensionless temperature decreases continuously from a maximum value at the surface of the plate to zero at the edge of the thermal boundary layer.

Fig. 4 shows that the surface temperature increases with the increase of the generalized Hartmann number due to the reduced fluid flow. Subsequently, increasing the Hartmann number increases the thermal boundary layer thickness and decreases the heat transfer rate, as presented in Fig. 5. Also, as expected, with the decrease of the generalized Prandtl number, the dimensionless temperature scale increases while the thermal boundary layer thickness decreases. However, variations with n depends on the value of Pr^* in which a lower n at $Pr^* = 1$ or 10 results in a larger temperature scale and a thicker thermal boundary layer, while the contrary result is obtained for $Pr^* = 0.1$. Similar to the variations of skin friction coefficient, the apparently contradictory trend of viscosity index functionality of temperature can be justified by the presence of the effect of the power index n on the velocity field.

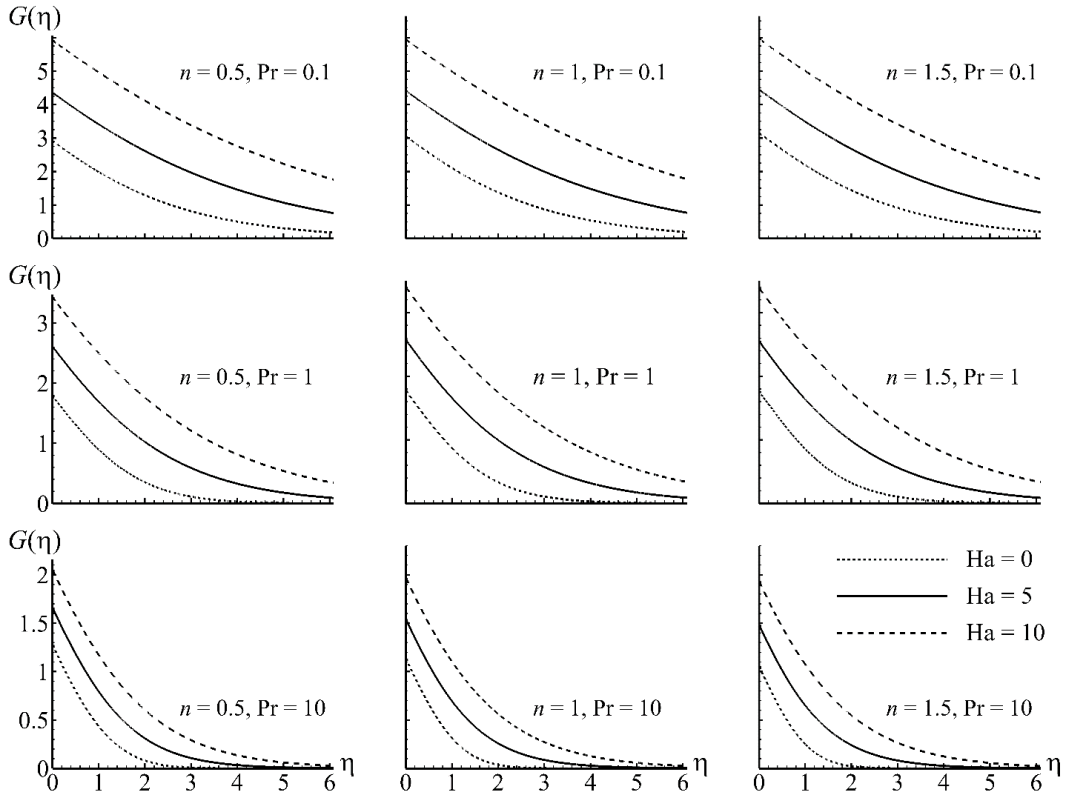

Fig. 4. Dimensionless temperature distribution for different n and Pr^* for $Ha^* = 0$, 5, and 10.

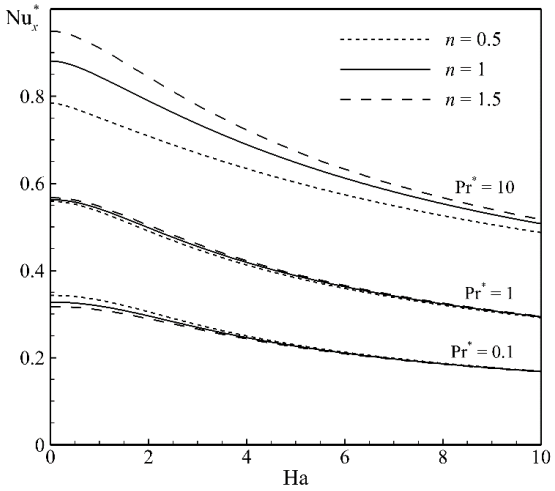

Fig. 5. Variations of dimensionless Nusselt number versus Ha for different values of Pr^* and n.

As presented in Fig. 5, the reverse trends are established for the variations of dimensionless Nusselt number with *n*, which is given by reciprocal of dimensionless wall temperature. As can be seen in Fig. 5, the Nusselt number has a weak decreasing functionality with viscosity index *n* for Pr^* = 0.1 and 1. This is resulted from the consequent effect of the Pr^* value and the magnitude of changes in the effective viscosity with index *n*. The weak functionality of Nusselt number with *n* is due to negligible effect of the velocity field at the edge of the thermal layer for low Pr^*.

The scale-ups between the viscous force, Lorentz force, and the inertia force propose a general correlation for the normalized Nusselt number in the form presented in Eq. (15). The least square method is employed using about 1,500 data from different curves of Pr^*–constant, Ha^*–constant, and *n*–constant. The following correlation for evaluating the Nusselt number is obtained for the ranges of $0.5 \leq n \leq 1.5$ and $0.1 \leq Pr \leq 10$ and $0 \leq Ha \leq 10$.

$$4.55\left(\frac{4.81}{Pr^*}\right)^n Nu_x^{*\,3n+3} + \frac{7.55}{Pr^{*2}} Nu_x^{*\,6} + 1.63\frac{Ha^2}{Pr^*} Nu_x^{*\,4} = 1 \qquad (15)$$

The correlation Eq. (15) calculates the value of the Nusselt number with the relative error up to 7% occurring around the point $Ha^* = 10$, $Pr^* = 0.1$, and $n = 0.5$. A comparison of the values of Nusselt number for Newtonian fluids with the results of Samanta and Guha [28] is presented in Tab. 1.

Tab. 1. Comparison of the results of Nusselt number for Newtonian fluids.

		Present study (for *n*=1)		Samanta and Guha [28]	
Pr	Ha	Numerical result	Correlation	Numerical result	Correlation
0.01	0	0.169	0.153	0.168	0.161
	3	0.149	0.136	0.148	0.135
0.7	0	0.522	0.527	0.522	0.542
	3	0.421	0.429	0.421	0.453
100	0	1.325	1.287	1.319	1.297
	3	1.157	1.209	1.159	1.083

4. Conclusion

The present work studied the MHD natural convection flow of power-law fluids over a horizontal plate with constant heat flux boundary condition. The flow was considered as steady, two-dimensional, laminar, and incompressible. The governing boundary layer equations were transformed to a set of ordinary differential equations using similarity transformation. The finite difference method was employed to solve the coupled ordinary differential equations for various values of generalized Hartmann number (Ha^*), generalized Prandtl number (Pr^*), and the non-Newtonian power-law viscosity index (*n*). A general correlation has been developed for Nusselt number using the numerical results. The flow and heat transfer characteristics show different behaviors from that of the Newtonian fluids. In summary, the important findings of the presented work are listed as follows.

The maximum value of the dimensionless velocity component along the plate decreases with the increase of the generalized Hartmann number. Moreover, the location of maximum velocity approaches the leading edge with the increase of the generalized Hartmann number. Generally, increasing the Hartmann number increases the boundary layer thickness; but, opposite trend was seen

when low Hartmann numbers are applied for the cases with thick boundary layers at high Pr^* and low *n* values.

The maximum value of the velocity component along the plate decreases with the increase of the generalized Prandtl number. However, increasing the power-law viscosity index results in a larger and sharper peak velocity but a thinner boundary layer thickness since the effective viscosity decreases in shear-thickening fluids and increases in the shear-thinning fluids by the decrease in the velocity gradient.

The wall skin friction coefficient decreases with the increase in Hartmann number especially at lower Pr^*. Increasing the Hartmann number increases the wall temperature and thermal boundary layer thickness and decreases the Nusselt number.

Decreasing the generalized Prandtl number increase the dimensionless skin friction, wall temperature, and thermal boundary layer thickness. Nevertheless, variations with the viscosity index depends on the value of the generalized Prandtl number in which decreasing the viscosity index at $Pr^* = 10$ increases the wall skin friction, temperature scale, and thermal boundary layer thickness, while the contrary results are obtained for $Pr^* = 0.1$. The reverse trends are established for the variations of dimensionless Nusselt numbers with *n*.

Acknowledgment

We would like to express our gratitude to the Semnan Branch, Islamic Azad University for their support regarding this research study.

Nomenclature

B − magnetic field ($=B_0 Gr_x^{*(n-2)/12}$), [T]

c_f − skin-friction coefficient, [–]

c_f^* − normalized skin-friction coefficient ($=\mathrm{Gr}_x^{*\frac{2-n}{6}} c_{f_x}$), [–]

F − dimensionless stream function, [–]

g − gravitational acceleration, [ms^{-2}]

G − dimensionless temperature, [–]

Gr^* − generalized Grashof number ($=g\beta q_w x^{\frac{4}{2-n}}/k\nu_0^{\frac{2}{2-n}}$), [–]

H − dimensionless pressure, [–]

Ha^* − generalized Hartmann number ($=B_0[g\beta q_w/k]^{-\frac{1}{4}}\sqrt{\sigma/\rho}$), [–]

k − fluid thermal conductivity, [$Wm^{-1}K^{-1}$]

L − length scale, [m]

n − non-Newtonian power-law index, [–]

Nu − Nusselt number ($=q_w x/[k(T_w(x)-T_\infty)]$), [–]

Nu^* − normalized Nusselt number ($=\mathrm{Gr}_x^{*\frac{n-2}{6}}\mathrm{Nu}_x$), [–]

p − static pressure, [Pa]

Pr^* − generalized Prandtl number ($=[\nu_0/\alpha][g\beta q_w/k]^{\frac{n-1}{2}}$), [–]

u, v − velocity components, [ms^{-1}]

x, y − coordinates, [m]

Greek Symbols

α − thermal diffusivity, [m^2s^{-1}]

β − thermal expansion coefficient, [K^{-1}]

η − dimensionless similarity variable, [–]

μ − dynamic viscosity, [Nsm^{-2}]

μ_0 − flow consistency index, [Ns^nm^{-2}]

ν_0 − reference kinematic viscosity, [m^2s^{n-2}]

ρ − density of fluid, [kgm^{-3}]

σ − electrical conductivity, [$A^2s^3kg^{-1}m^{-3}$]

τ_w − wall shear stress, [Pa]

ψ − stream function, [m^2s^{-1}]

Subscripts

w − value related to the plate surface

x − local value

q_w − surface heat flux, [Wm^{-2}]

T − temperature, [K]

∞ − ambient condition

δ − value related to the boundary layer edge

References

[1] Martynenko, O. G., and Khramtsov, P. P., Free-convective heat transfer, Springer-Verlag, Berlin, Germany, ISBN: 978-3-540-28498-7, 2005

[2] Pretot, S., *et al*., Theoretical and experimental study of natural convection on a horizontal plate, *Applied Thermal Engineering, 20* (2000), 10, pp. 873-891

[3] Samie, M., *et al*., Two-dimensional free convection heat transfer below a horizontal hot isothermal flat strip, *Journal of Heat Transfer, 137* (2015), 5, pp. 052503.1-052503.10

[4] Kozanoglu, B., Rubio, F., The characteristic length on natural convection from a horizontal heated plate facing downwards, *Thermal Science, 18* (2014), 2, pp. 555–561

[5] Samanta, S., Guha, A., A similarity theory for natural convection from a horizontal plate for prescribed heat flux or wall temperature, *International Journal of Heat and Mass Transfer, 55* (2012), 13-14, pp. 3857-3868

[6] Mehrizi, A. A., *et al*., New analysis of natural convection boundary layer flow on a horizontal plate with variable wall temperature, *Journal of Theoretical and Applied Mechanics, 50* (2012), 4, pp. 1001-1010

[7] Guha, A., Samanta, S., Closed-form analytical solutions for laminar natural convection on horizontal plates, *Journal of Heat Transfer, 135* (2013), 10, pp. 102501.1-102501.9

[8] Moulic, S. G., Yao, L. S., Non-Newtonian natural convection along a vertical flat plate with uniform surface temperature, *Journal of Heat Transfer, 131* (2009), 6, pp. 062501.1-062501.8

[9] Molla, M. M., Yao, L.-S., Non-Newtonian natural convection along a vertical plate with uniform surface heat fluxes, *Journal of Thermophysics and Heat Transfer, 23* (2009), 1, pp. 176-185

[10] Capobianchi, M., Aziz, A., Laminar natural convection between a vertical surface with uniform heat flux and pseudoplastic and dilatant fluids, *Journal of Heat Transfer, 136* (2014), 9, pp. 092501.1-092501.9

[11] Ece, M. C., Büyük, E., Similarity solutions for free convection to power-law fluids from a heated vertical plate, *Applied Mathematics Letters, 15* (2002), 1, pp. 1-5,

[12] Abolfazli Esfahani, J., Bagherian, B., Similarity solution for unsteady free convection from a vertical plate at constant temperature to power law fluids, *Journal of Heat Transfer, 134* (2012), 10, pp. 102501.1-102501.7

[13] Sui, J., *et al*., Convection heat transfer of power-law fluids along the inclined nonuniformly heated plate with suction or injection, *Journal of Heat Transfer, 138* (2015), 2, pp. 021701.1-021701.1

[14] Chen, H. T., Chen, C. K., Natural convection of non-Newtonian fluids about a horizontal surface in a porous medium, *Journal of Energy Resources Technology, 109* (1987), 3, pp. 119-123

[15] Gorla, R. S. R., Kumari, M., Nonsimilar solutions for free convection in non-Newtonian fluids along a horizontal plate in a porous medium, *International Journal of Fluid Mechanics Research, 31* (2004), 2, pp. 116-130

[16] Guha, A., Pradhan, K., Natural convection of non-Newtonian power-law fluids on a horizontal plate, *International Journal of Heat and Mass Transfer, 70* (2014), pp. 930-938

[17] Kabeel, A.E., *et al*., A review of magnetic field effects on flow and heat transfer in liquids: Present status and future potential for studies and applications, *Renewable and Sustainable Energy Reviews, 45* (2015), pp. 830-837

[18] Ashouri, M., *et al*., MHD natural convection flow in cavities filled with square solid blocks, *International Journal of Numerical Methods for Heat and Fluid Flow, 24* (2014), pp. 1813-1830

[19] Touihri, R., *et al*., Instabilities in a cylindrical cavity heated from below with a free surface. II. Effect of a horizontal magnetic field, *Physical Review E, 84* (2011), pp. 056303.1-13

[20] Mostaghimi, P., *et al*., Hydrodynamics of fingering instability in the presence of a magnetic field, *Fluid Dynamics Research, 48* (2016), pp. 055504-055519

[21] Chen, C-T., Thermal instability in natural convection flow over a boundary layer subject to external electrical and magnetic fields, *Heat and Mass Transfer, 45* (2009), pp. 1589-1596

[22] Sangapatnam, S., *et al*., Radiation and Mass Transfer Effects on MHD Free Convection Flow Past an Impulsively Started Isothermal Vertical Plate with Dissipation, *Thermal Science, 13* (2009), 2, 171-181

[23] Huang, C-J., Influence of non-Darcy and MHD on free convection of non-Newtonian fluids over a vertical permeable plate in a porous medium with soret/dufour effects and thermal radiation, *International Journal of Thermal Sciences, 130* (2018), pp. 256-263

[24] Tak, S. S., *et al*., MHD free convection-radiation interaction along a vertical surface embedded in Darcian porous medium in presence of Soret and Dufour's effects, *Thermal Science, 14* (2010), 1, 137-145

[25] Parasuraman, L., *et al*., Radiation effects on an unsteady MHD natural convective flow of a nanofluid past a vertical plate, *Thermal Science, 19* (2015), 3, 1037-1050

[26] El-Amin, M. F., Combined effect of magnetic field and viscous dissipation on a power-law fluid over plate with variable surface heat flux embedded in a porous medium, *Journal of Magnetism and Magnetic Materials, 261* (2003), 1–2, pp. 228-237

[27] Mehta, K. N., Rao, K. N., Buoyancy induced flow of non-newtonian fluids over a non-isothermal horizontal plate embedded in a porous medium, *International Journal of Engineering Science, 32* (1994), 3, pp. 521-525

[28] Samanta, S., Guha, A., Analysis of heat transfer and stability of magnetohydrodynamic natural convection above a horizontal plate with heat flux boundary condition, *International Journal of Heat and Mass Transfer, 70* (2014), pp. 793-802

[29] Bahmani, A., Kargarsharifabad, H., Laminar natural convection of power-law fluids over a horizontal heated flat plate, *Heat Transfer – Asian Research,* (2019), doi:10.1002/htj.21420.